

Gas-Phase Reactions of Atomic Lanthanide Cations with D₂O: Room-Temperature Kinetics and Periodicity in Reactivity

Ping Cheng, Gregory K. Koyanagi, and Diethard K. Bohme*^[a]

Reactions of atomic lanthanide cations (excluding Pm⁺) with D₂O have been surveyed in the gas phase using an inductively coupled plasma/selected-ion flow tube (ICP/SIFT) tandem mass spectrometer to measure rate coefficients and product distributions in He at 0.35 ± 0.01 Torr and 295 ± 2 K. Primary reaction channels were observed corresponding to O-atom transfer, OD transfer and D₂O addition. O-atom transfer is the predominant reaction channel and occurs exclusively with Ce⁺, Nd⁺, Sm⁺, Gd⁺, Tb⁺ and Lu⁺. OD transfer is observed exclusively with Yb⁺, and competes with O-atom transfer in the reactions with La⁺ and Pr⁺. Slow D₂O addition is observed with early lanthanide cation Eu⁺ and the late lanthanide cations Dy⁺, Ho⁺, Er⁺ and Tm⁺. Higher-order sequential D₂O addition of up to five D₂O molecules is observed with LnO⁺ and LnOD⁺. A delay of more than 50 kcal mol⁻¹ is observed in the onset of efficient exothermic O-

atom transfer, which suggests the presence of kinetic barriers of perhaps this magnitude in the exothermic O-atom transfer reactions of Dy⁺, Ho⁺, Er⁺ and Tm⁺ with D₂O. The reaction efficiency for O-atom transfer is seen to decrease as the energy required to promote an electron to make two non-f electrons available for bonding increases. The periodic trend in reaction efficiency along the lanthanide series matches the periodic trend in the electron-promotion energy required to achieve a d¹s¹ or d² excited electronic configuration in the lanthanide cation, and also the periodic trends across the lanthanide row reported previously for several alcohols and phenol. An Arrhenius-like correlation is also observed for the dependence of D₂O reactivity on promotion energy for early lanthanide cations, and exhibits a characteristic temperature of 2600 K.

1. Introduction

The long-neglected lanthanide elements are gaining importance in many areas of modern technology.^[1] Parallel to the increasing industrial use of lanthanides, an increasing interest has developed in the ion chemistry of the lanthanide elements.^[2] Studies into the gas-phase reactivities of isolated lanthanide cations began in the late 1980s with Fourier-transform (FT) mass spectrometry and various ion-beam techniques, together with laser ablation to produce the atomic cations.^[3] Numerous investigations over the past 20 years have made available extensive data on the gas-phase reactions of the lanthanide cations (Ln⁺) with various inorganic and organic molecules including hydrogen,^[4] oxygen and nitrous oxide,^[5] alkanes and cycloalkanes,^[3b,c,6] alkenes,^[3a,b,7] alcohols,^[8] benzene and substituted benzenes,^[9] phenol,^[10] orthoformates,^[9a,11] ferrocene and Fe pentacarbonyl,^[12] methyl fluoride^[13] and methyl chloride.^[14] Generally, these studies show that the reactivity of Ln⁺ varies along the 4f series in terms of both the ionic products formed and the reaction efficiencies. These variations have been related to the accessibility of excited electron configurations with two unpaired non-f electrons, that is, to the energies required to excite the ground states of the Ln⁺ cations, typically from 4fⁿ5d⁰6s¹ to the 4fⁿ⁻¹5d¹6s¹ states. A recent bonding configuration analysis by Gibson^[15] suggests that two unpaired 5d valence electrons, rather than a 5d and a 6s electron, affect the bonding between the metal centre and the oxygen atom in LnO⁺. The variations in the promotion ener-

gies required to achieve either 5d² or 5d¹6s¹ excitation are qualitatively similar across the Ln⁺ cations, and result in similar predictions for the periodic and Arrhenius-like dependencies of the efficiencies of O-atom transfer on the electron-promotion energy, except for differences in characteristic temperature.

To extend these basic investigations, herein we present a general survey of the gas-phase reactions of Ln⁺ with D₂O (excluding Pm⁺). We chose D₂O rather than H₂O to improve the product-ion mass resolution. Surprisingly, to the best of our knowledge, there are no previous reports on the reactions of Ln⁺ with water, although gas-phase reactions between water and other metal cations have been surveyed by several groups.^[16] As early as 1971, Biondi et al.^[17] reported the first measurement of the reactions of K⁺ and Na⁺ with water. Reactions of first-row transition metal cations with water have been surveyed by the Armentrout research group^[16b,18] using guided ion-beam mass spectrometry. Ugalde et al.^[19] have analysed reactions of first-row transition metal cations with water by employing ab initio theory. Our own recent investigations of the reactions of almost all of the first-, second- and third-row tran-

[a] Dr. P. Cheng, G. K. Koyanagi, Prof. D. K. Bohme
Department of Chemistry, Centre for Research in Mass Spectrometry and
Centre for Research in Earth and Space Science
York University, Toronto, Ontario, M3J 1P3 (Canada)
Fax: (+1) 416-736-5936
E-mail: dkbohme@yorku.ca

sition metal cations in the periodic table with D_2O will be reported separately.^[20]

In the experimental studies reported here, all Ln^+ cations are formed within the same source, an inductively coupled plasma (ICP) of argon at 5500 K. The ions are allowed to react with D_2O at room temperature (295 ± 2 K) in helium buffer gas (0.35 ± 0.1 Torr) and the reactions are monitored by selected ion flow tube (SIFT) tandem mass spectrometry.^[5,21] Primary reaction rate coefficients and reaction product distributions are measured and subsequent reactions are followed as well.

Experimental Section

The experimental results reported here were obtained with the ICP/SIFT tandem mass spectrometer that has been described in detail previously.^[5,21] The atomic ions were generated within an atmospheric-pressure argon plasma at 5500 K fed with a vaporized solution containing the lanthanide salt. Solutions containing the metal salt of interest at a concentration of approximately $5 \mu\text{g L}^{-1}$ were peristaltically pumped via a nebulizer into the plasma. The plasma gas flow was adjusted to maximize the ion signal detected downstream of the SIFT. The sample solutions were prepared using atomic spectroscopy standard solutions commercially available from SPEX, Teknolab, J.T. Baker Chemical Co., Fisher Scientific Company, Perkin–Elmer and Alfa Products. The ions emerging from the ICP were injected through a differentially pumped sampling interface into a quadrupole mass filter and, after mass analysis, introduced through an aspirator-like interface into flowing helium carrier gas at 0.35 ± 0.01 Torr and 295 ± 2 K. After experiencing about 10^5 collisions with He atoms, the ions were allowed to react with D_2O added into the flow tube.

The lanthanide ions emerging from the plasma initially had a Boltzmann internal energy distribution characteristic of the plasma temperature. However, these emerging populations are expected to be downgraded during the ≈ 20 ms duration before entry into the reaction region in the flow tube. Energy degradation can occur by radiative decay as well as by collisions with argon atoms and the 10^5 collisions with He before entry into the reaction region. The electronic states of the lanthanides, due to the presence of f electrons, are a mixture of states with both positive and negative parity. This means that there are a large number of parity-allowed transitions that occur quickly ($\approx 10^{-8}$ s), thus changing their original state distribution from the ICP. La^+ itself is an exception for lanthanides in that it behaves like a transition metal ion, since it does not have any low-lying states with occupied f orbitals. The extent to which quenching of any electronically excited states of the lanthanide cations that may be formed within the ICP is complete is uncertain, and could be inferred only indirectly from the observed decays of primary ion signals. The observed semi-logarithmic decays of the reacting lanthanide cations were invariably linear over as much as three decades of ion depletion and so were indicative of single-state populations (or multiple-state populations with equal reactivities). The many collisions with Ar and He between the source and the reaction region should ensure that the atomic ions reach a translational tem-

perature equal to the tube temperature of 295 ± 2 K prior to entering the reaction region.

Reactant and product ions were sampled at the end of the flow tube with a second quadrupole mass filter and their signals were measured as a function of added reactant. The resulting profiles provide information about reaction rate coefficients and product ion distributions. Rate coefficients for primary reactions are determined with an uncertainty estimated to be less than $\pm 30\%$ from the semi-logarithmic decay of the reactant-ion intensity as a function of added reactant.

D_2O was introduced into the reaction region of the SIFT as a dilute mixture in helium ($\approx 2.5\%$) and obtained commercially with high purity (Aldrich, isotopic purity > 99.75 at $\% \pm D$).

2. Results and Discussion

The reactions of 14 lanthanide cations with D_2O are investigated and both the primary and higher-order chemistries are monitored. All lanthanide cations exhibit some reactivity towards D_2O , mostly resulting in LnO^+ formation. The results obtained for the reactions of La^+ , Ce^+ , Gd^+ and Lu^+ are shown in Figure 1. Table 1 summarizes the measured rate coefficients and product distributions and derived reaction efficiencies. The reaction efficiency is taken to be equal to the ratio k/k_c where

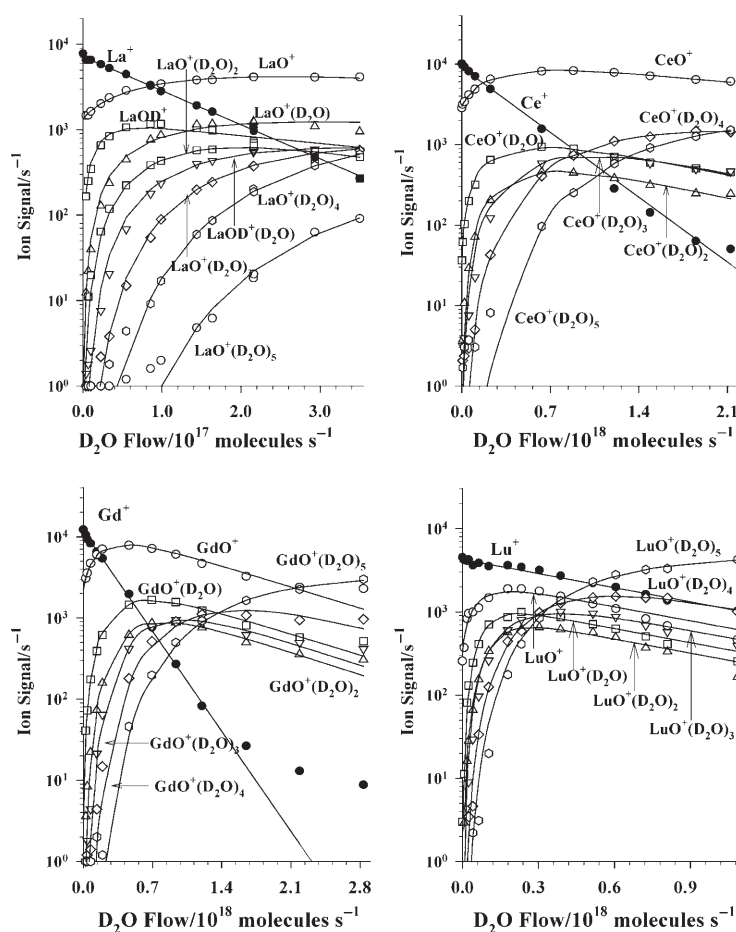


Figure 1. Composite of ICP/SIFT results for the reactions of the lanthanide cations Ce^+ , Pr^+ , Gd^+ and Lu^+ with D_2O in helium buffer gas at 0.35 ± 0.01 Torr and 295 ± 2 K.

Table 1. Primary reaction rate coefficients, primary product distributions and higher-order product ions measured for reactions of atomic cations Ln⁺ with D₂O in helium at 0.35 ± 0.01 Torr and 295 ± 2 K. Also included are calculated collision rate coefficients and the derived reaction efficiencies (k/k_c).

M ⁺	$k^{[a]}$	$k_c^{[b]}$	k/k_c	Primary products	PD ^[c]	Higher-order product ions
La ⁺	3.0	21.3	0.14	LaO ⁺ LaOD ⁺	80 20	LaO ⁺ (D ₂ O) ₁₋₅ LaOD ⁺ (D ₂ O)
Ce ⁺	2.0	21.3	9.5 × 10 ⁻²	CeO ⁺	100	CeO ⁺ (D ₂ O) ₁₋₅
Pr ⁺	0.1	21.3	4.3 × 10 ⁻³	PrO ⁺ PrOD ⁺	95 5	PrO ⁺ (D ₂ O) ₁₋₅
Nd ⁺	0.02	21.3	1.0 × 10 ⁻³	NdO ⁺	100	NdO ⁺ (D ₂ O) ₁₋₅
Sm ⁺	0.013	21.2	6.7 × 10 ⁻⁴	SmO ⁺	100	SmO ⁺ (D ₂ O) ₁₋₅
Eu ⁺	≤ 0.005	21.2	≤ 2.4 × 10 ⁻⁴	Eu ⁺ (D ₂ O)	100	
Gd ⁺	2.3	21.2	0.11	GdO ⁺	100	GdO ⁺ (D ₂ O) ₁₋₅
Tb ⁺	0.82	21.2	0.04	TbO ⁺	100	TbO ⁺ (D ₂ O) ₁₋₅
Dy ⁺	≤ 0.005	21.1	≤ 2.4 × 10 ⁻⁴	Dy ⁺ (D ₂ O)	100	
Ho ⁺	≤ 0.005	21.1	≤ 2.4 × 10 ⁻⁴	Ho ⁺ (D ₂ O)	100	
Er ⁺	≤ 0.005	21.1	≤ 2.4 × 10 ⁻⁴	Er ⁺ (D ₂ O)	100	
Tm ⁺	≤ 0.005	21.1	≤ 2.4 × 10 ⁻⁴	Tm ⁺ (D ₂ O)	100	
Yb ⁺	0.052	21.0	2.5 × 10 ⁻³	YbO ⁺	100	YbOD ⁺ (D ₂ O) ₁₋₅
Lu ⁺	0.7	21.0	3.5 × 10 ⁻²	LuO ⁺	100	LuO ⁺ (D ₂ O) ₁₋₅

[a] Measured reaction rate coefficient (in units of 10⁻¹⁰ cm³ molecule⁻¹ s⁻¹) with an estimated accuracy of ± 30%. [b] Calculated capture rate coefficient in units of 10⁻¹⁰ cm³ molecule⁻¹ s⁻¹. [c] PD = primary product distribution expressed as a percentage.

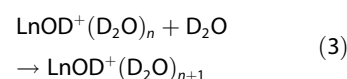
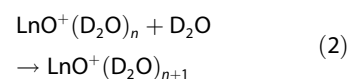
k is the experimentally measured rate coefficient and k_c is the capture or collision rate coefficient. The value of k_c is computed using the algorithm of the modified variational transition-state/classical trajectory theory developed by Su and Chesnavich^[22] with $\alpha(\text{D}_2\text{O}) = 1.26 \times 10^{-24} \text{ cm}^3$ ^[23] and $\mu_D(\text{D}_2\text{O}) = 1.8545 \text{ D}$.^[24]

The three primary reaction channels that are observed are indicated in Reactions (1a–1c):



They correspond to bimolecular O-atom transfer [Reaction (1a)], bimolecular OD group transfer [Reaction (1b)] and D₂O addition [Reaction (1c)]. O-atom transfer is the predominant reaction channel and was seen in the reactions with La⁺, Ce⁺, Pr⁺, Nd⁺, Sm⁺, Gd⁺, Tb⁺ and Lu⁺. OD group transfer was the only channel observed with Yb⁺ and competed with O-atom transfer in the reactions with La⁺ and Pr⁺. D-atom transfer is not observed, probably due to the low D-atom affinities of the Ln⁺ cations, cf. H-atom affinities HA(La⁺) = 57.2 ± 2.1 kcal mol⁻¹, HA(Lu⁺) = 48.6 ± 3.7 kcal mol⁻¹,^[4] these are both smaller than the value for HA(OH) (see Table 3). D₂O addition is seen with the late lanthanide cations Dy⁺, Ho⁺, Er⁺ and Tm⁺ and the early lanthanide cation Eu⁺, but the reaction rates are very low and the corresponding reaction rate coefficients are all below our instrumental measuring limit. As expected from the much lower first ionization energy of the lanthanides [IE(Ln)], which are all < 6.3 eV, compared with that for D₂O (12.6395 ± 0.0003 eV),^[25] electron transfer is not observed with any of the Ln⁺ cations.

The secondary and higher-order reactions that are observed all correspond to D₂O addition. No secondary O-atom abstraction is observed with the primary product LnO⁺ to produce LnO₂⁺. The D₂O is observed to hydrate almost all of the monoxide and hydroxide lanthanide cations according to Reactions (2) and (3):



All these addition reactions are expected to proceed in a termolecular fashion under our experimental operating conditions,

with He buffer-gas atoms acting as the stabilizing third body.

Secondary and higher-order D₂O addition is observed for LnO⁺ = LaO⁺ ($n=0-4$), CeO⁺ ($n=0-4$), PrO⁺ ($n=0-4$), NdO⁺ ($n=0-4$), SmO⁺ ($n=0-4$), GdO⁺ ($n=0-4$), TbO⁺ ($n=0-4$) and LuO⁺ ($n=0-4$), and LnOD⁺ = LaOD ($n=0$) and YbOD⁺ ($n=0-4$). We did not see the higher-order D₂O adducts Ln⁺(D₂O) _{n} ($n > 1$), probably because of the small initial rate of formation of Ln⁺(D₂O).

2.1. Periodicities in Reaction Efficiency

The efficiencies of the 14 primary reactions of Ln⁺ cations with D₂O change dramatically along the 4f row and range from < 2.4 × 10⁻⁴ (Eu⁺) to 0.14 (La⁺). The efficiencies of O-atom transfer with La⁺ (5d²), Ce⁺ (4f¹5d²) and Gd⁺ (4f⁷5d¹6s¹) are all relatively high at about 10%, and it is interesting to note that these particular cations all have two unpaired non-f electrons in their electronic ground state and are the only ones that have such electrons [Lu⁺ (4f¹⁴5s²) has a filled s orbital]. In contrast, the efficiencies of the other O-atom transfer reactions of Pr⁺ (0.004), Nd⁺ (0.001), Sm⁺ (0.00067), Tb⁺ (0.04) and Lu⁺ (0.035) are all ≤ 0.04. The efficiencies for OD group transfer to La⁺, Pr⁺ and Yb⁺ are 0.028, 0.0002 and 0.0025, respectively. The reaction rates for D₂O addition are very slow and the efficiencies with Eu⁺, Dy⁺, Ho⁺, Er⁺ and Tm⁺ are all ≤ 2.4 × 10⁻⁴, below the detection limit. An overview of the variation in reaction efficiency of O-atom transfer across the lanthanide series is included in Figure 2.

2.2. Thermodynamics of O-Atom and OD Group Transfer

The O-atom affinities (OAs) listed in Table 2 indicate that all but three of the 14 lanthanide cations investigated have OA-

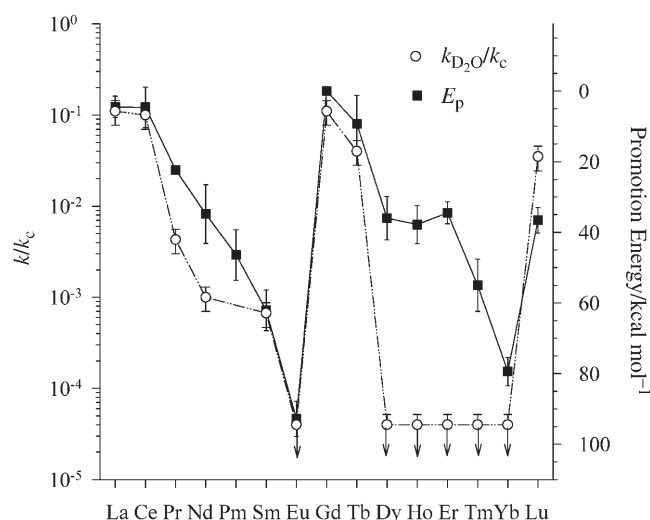


Figure 2. O-atom transfer reaction efficiency (\circ and left ordinate axis) and the energy required to promote an electron and leave the Ln^+ cation in a d^1s^1 configuration (\blacksquare and right ordinate axis) plotted along the lanthanide row of elements.

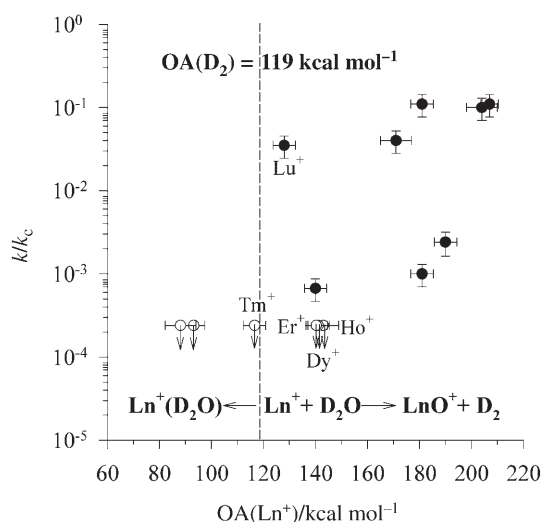


Figure 3. Dependence of the reaction efficiency (k/k_c) on the O-atom affinity (OA) of the Ln^+ cation. Reactions on the right of the dashed line are exothermic for O-atom transfer while those on the left are endothermic. (\circ) D_2O addition reactions; (\bullet) O-atom abstraction reactions.

Ln^+ species	OA(Ln^+)	Ln^+ ground-state valence configuration	Ln^+ term symbol	Promotion energy to first $5d^16s^1$ configuration
La^+	206.6 ± 3.4	$5d^2$	3F_2	4.5 ± 3.0
Ce^+	203.6 ± 5.9	$4f^15d^2$	$^4H_{7/2}^0$	4.6 ± 5.7
Pr^+	189.6 ± 4.3	$4f^36s^1$	$(9/2, 1/2)_4^0$	22.3 ± 0.8
Nd^+	180.8 ± 4.3	$4f^46s^1$	$^6I_{7/2}$	34.8 ± 8.3
Pm^+		$4f^56s^1$	$^7H_2^0$	46.4 ± 7.2
Sm^+	139.6 ± 4.3	$4f^66s^1$	$^8F_{7/2}$	62.1 ± 5.8
Eu^+	93.2 ± 4.3	$4f^76s^1$	$^9S_4^0$	92.8 ± 5.0
Gd^+	180.6 ± 4.3	$4f^75d^16s^1$	$^{10}D_{5/2}^0$	0.0
Tb^+	171.0 ± 5.9	$4f^96s^1$	$(15/2, 1/2)_8^0$	9.3 ± 8.1
Dy^+	143.3 ± 5.9	$4f^{10}6s^1$	$(8, 1/2)_{17/2}$	36.0 ± 6.1
Ho^+	141.3 ± 4.3	$4f^{11}6s^1$	$(15/2, 1/2)_8^0$	37.8 ± 5.4
Er^+	140.3 ± 4.3	$4f^{12}6s^1$	$(6, 1/2)_{13/2}$	34.5 ± 3.1
Tm^+	116.6 ± 4.3	$4f^{13}6s^1$	$(7/2, 1/2)_4^0$	55.5 ± 7.4
Yb^+	88.1 ± 5.9	$4f^{14}6s^1$	$^2S_{1/2}$	79.4 ± 4.0
Lu^+	128.0 ± 4.3	$4f^{14}6s^2$	1S_0	36.6 ± 3.6

(Ln^+) > $\text{OA}(\text{D}_2) = 119.2 \text{ kcal mol}^{-1}$. So O-atom transfer is exothermic in 11 cases. However, our measurements indicate a wide range of reactivity (see Figure 3), which shows how the reaction efficiency varies with O-atom affinity.

O-atom abstraction is the predominant reaction channel with only eight of these 11 cations (La^+ , Ce^+ , Pr^+ , Nd^+ , Sm^+ , Gd^+ , Tb^+ and Lu^+), and proceeds with rate coefficients in the range from 1.3×10^{-12} (Sm^+) to $2.4 \times 10^{-10} \text{ cm}^3 \text{ molecule}^{-1} \text{ s}^{-1}$ (La^+). The three late lanthanide metal cations, all with O-atom affinities greater than $\text{OA}(\text{D}_2)$, Dy^+ ($143.3 \text{ kcal mol}^{-1}$), Ho^+ ($141.3 \text{ kcal mol}^{-1}$) and Er^+ ($140.3 \text{ kcal mol}^{-1}$), do not exhibit O-atom transfer ($k \leq 5 \times 10^{-13} \text{ cm}^3 \text{ molecule}^{-1} \text{ s}^{-1}$). Clearly O-atom

transfer is not thermodynamically controlled. With the exception of Lu^+ , Figure 3 shows a delay of more than 50 kcal mol^{-1} in the onset of efficient exothermic O-atom transfer. Energy barriers inhibit most O-atom transfer reactions less exothermic than 50 kcal mol^{-1} .

For OD group transfer to be exothermic, the OD affinity (ODA) of the lanthanide cation must exceed $\text{ODA}(\text{D}) = 121.3 \text{ kcal mol}^{-1}$ ^[25]. The OD affinities for the 14 lanthanide cations that are studied appear to be unavailable at present. However, our observation of OD transfer in the reactions with La^+ , Pr^+ and Yb^+ suggests that the OD affinities of these atomic cations are $\geq 121.3 \text{ kcal mol}^{-1}$. The reaction with Yb^+ is an interesting special case since it leads only to YbOD^+ with an efficiency of 2.5×10^{-3} . O-atom transfer is the most endothermic (by $29.4 \text{ kcal mol}^{-1}$) with this lanthanide cation. Apparently $\text{ODA}(\text{Yb}^+) > \text{ODA}(\text{D}) = 121.3 \text{ kcal mol}^{-1}$ (see Table 3) but this is not the case for the other lanthanide cations (Eu^+ , Dy^+ , Ho^+ , Er^+ and Tm^+), for which O-atom transfer is thermodynamically or kinetically unfavourable and with which only D_2O addition is observed.

Table 3. The bond energies $D(\text{X-OH})$ and $D(\text{XO-H})$ and the O-atom affinity $\text{OA}(\text{XH})$ for D_2O , methanol, ethanol, 2-propanol and phenol [kcal mol^{-1}].

Molecule, XOH	OA(XH)	$D(\text{XO-H})$	$D(\text{X-OH})$
D_2O ^[a]	119.2	121.3	121.3
methanol ^[a]	89.8	104.3 ± 1.0	92.5
ethanol ^[b]	95.6 ± 0.2	104.3 ± 1.0	93.7 ± 1.0
2-propanol ^[b]	99.8 ± 0.2	104.7 ± 1.0	96.8 ± 0.7
phenol ^[b]	102.5 ± 0.3	88.1 ± 1.7	113.4 ± 1.9

[a] Determined from the ΔH_f^0 found in ref. [25]. [b] Determined from the ΔH_f^0 found in ref. [27].

2.3. Correlation between Reactivities and Promotion Energies

We have seen that eight among the 14 lanthanide cations react with D₂O at room temperature via O-atom transfer. La⁺ (4f⁷5d¹6s¹) with two natural non-f valence electrons exhibits the highest efficiency for O-atom abstraction, followed closely by Gd⁺ (5d²) and Ce⁺ (4f¹⁴5d²). These three cations all have two non-f valence electrons. The reactivities of the remaining Ln⁺ cations (excluding Lu⁺ (4f¹⁴6s²)), all of which have available only one non-f electron (s¹), are all less and decrease along the early and late lanthanide series.

Figure 2 shows that the reaction efficiency for O-atom transfer follows quite closely the variation across the lanthanide row in the energy required to promote an f electron to achieve a 5d¹6s¹ configuration. Previously, we found this to be the case for some lanthanide cation reactions.^[5,13,14] Such a promotion would make two electrons available for bonding with atomic oxygen. Promotion to a 5d² configuration would achieve the same result and the variation in electron-promotion energy across the lanthanide row would be similar. Gibson^[15] has suggested that two unpaired 5d valence electrons, rather than a 5d and a 6s electron, affect the bonding between the metal centre and the oxygen atom in LnO⁺. Our observation of the approximately equal reactivity of 10% for the reactions of D₂O with Gd⁺(d¹s¹) on the one hand, and with La⁺(d²) and Ce⁺(d²) on the other, does not allow a distinction between these two possibilities. The values of the 4fⁿ6s¹ to 4fⁿ⁻¹5d¹6s¹ promotion energy for all 14 Ln⁺ cations are listed in Table 2. Lu⁺ should be regarded as an exception to the lanthanide cation series in that a 6s electron rather than a 4f electron is promoted to a 5d orbital.

Figures 4 and 5, the latter an Arrhenius-like plot, demonstrate that the measured reaction efficiency (k/k_c) at constant temperature (295 K) exhibits an exponential dependence on the promotion energy (E_p) according to Equations (4) and (5):

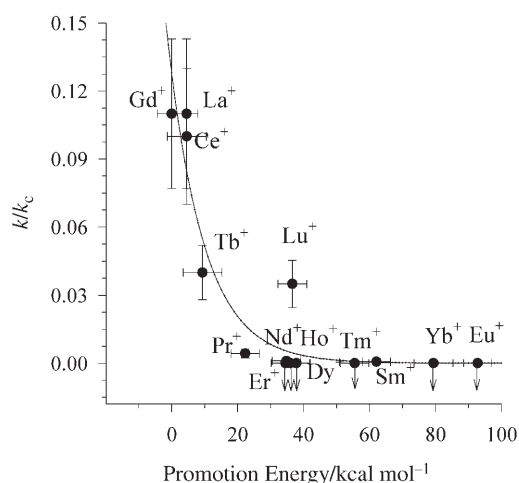


Figure 4. Correlation of reaction efficiency for O-atom abstraction from D₂O with the energy E_p required to promote an electron and leave the Ln⁺ cation in a d¹s¹ configuration. The curve represents a fit with $k/k_c = 0.074 \exp(-0.084E_p)$.

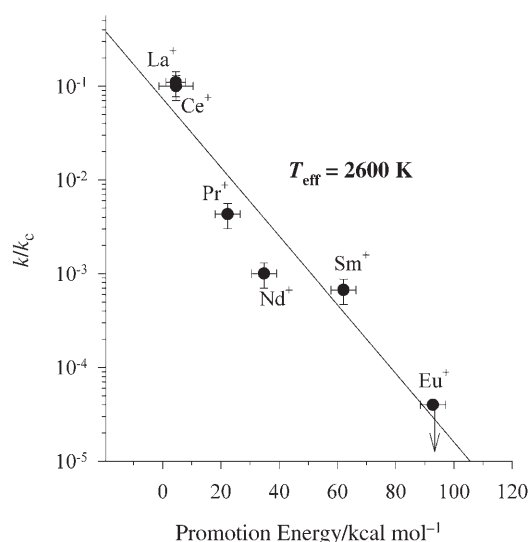


Figure 5. Arrhenius-like correlation of reaction efficiency for O-atom abstraction from D₂O with the energy required to promote an electron and leave the Ln⁺ in a d¹s¹ configuration.

$$k/k_c = 0.074 \exp(-0.084E_p) \quad (4)$$

$$k/k_c = \exp(-XE_p) \quad (5)$$

Lu⁺ clearly is anomalous in Figure 4 in that its reactivity is abnormally high and this is because a 6s electron rather than a 4f electron is promoted to a 5d orbital. The data set for Figure 5 is too limited for the late Ln⁺ cations; only three of these cations react with D₂O by O-atom transfer, including the special Lu⁺ (4f¹⁴6s²) cation, and so are not included in Figure 5. If X in Equation (5) is interpreted as $1/RT_{\text{eff}}$, the slope of the semi-logarithmic plot in Figure 5 indicates a characteristic temperature of 2600 ± 100 K for O-atom transfer reactions.

2.4. Comparison with the Ln⁺ Chemistry of Alcohols and Phenol

We can compare our results with those reported previously for some other monohydroxide-containing molecules, namely various alcohols and phenol. Fourier transform ion cyclotron resonance (FTICR) mass spectrometry, in which atomic ions are produced by laser ionization of pure metal pieces, has been employed to investigate reactions of lanthanide cations with methanol, ethanol, 2-propanol and phenol.^[8c,10] The reaction efficiencies determined with these four molecules are all higher than those obtained here with D₂O, but all show the same periodic variation across the lanthanide row that is observed with D₂O. The comparison is shown graphically in Figure 6. The order in total reaction efficiency, phenol > 2-propanol > ethanol > methanol > D₂O, can be attributed to the relative strength of the electrostatic interaction due to ion-dipole and ion-induced dipole interactions, as has been done previously for the three alcohols by Carretas et al.^[8c] These authors pointed to the increased availability of chemical activation energy with increasing electrostatic interaction in the order of

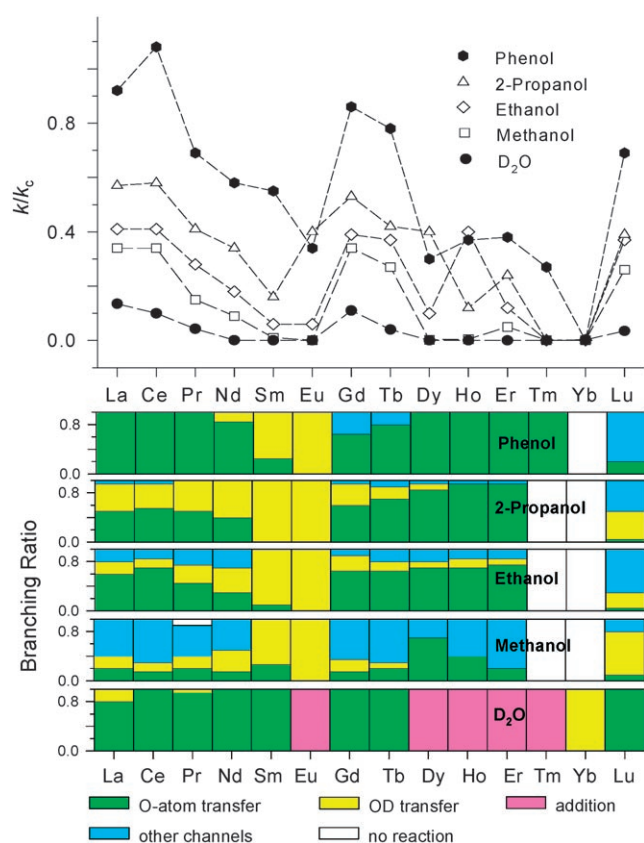


Figure 6. Comparison of experimental results obtained for total reaction efficiencies (top) and product branching fractions (bottom) for reactions of lanthanide cations with D_2O , methanol, ethanol, 2-propanol and phenol.

the polarizabilities of the three alcohols: methanol (3.29 \AA^3) < ethanol (5.41 \AA^3) < 2-propanol (7.61 \AA^3) where the polarizability of the alcohol is given in parentheses.^[26] D_2O (1.26 \AA^3) and phenol (11.1 \AA^3) fall at the two extremes of this range and so also fit this trend.

Also shown in Figure 6 are the measured product branching fractions for the Ln^+ reactions that are observed. All five molecules exhibit multiple products; D_2O shows the fewest and methanol the most different ionic products. All five molecules exhibit some O-atom transfer for which the exothermicity order is methanol > ethanol > 2-propanol > phenol > D_2O , with O-atom transfer from methanol being the most exothermic (see Table 3). The same exothermicity order applies to OH transfer (see Table 3). Competition between O and OH transfer is evident (except for the reactions with D_2O) and most noticeable for the reactions with 2-propanol. Other channels compete in the reactions with the lower alcohols and prevail with methanol, which produces $LnOCH_2^+$ (by H_2 elimination) and $LnOCH_3^+$ (by H elimination) in addition to LnO^+ and $LnOH^+$, all of which involve $Ln-O$ bond formation. Addition by collisional stabilization is more favourable under our SIFT conditions ($P_{He} = 0.35 \text{ Torr}$) than under FTICR conditions ($P = 10^{-5} \text{ Torr}$) and this accounts for the observation of this channel only in our experiments.

Notably, OD abstraction by Yb^+ is observed only in our SIFT experiments with D_2O , albeit with a very low rate coefficient,

$k = 5.2 \times 10^{-12} \text{ cm}^3 \text{ molecule}^{-1} \text{ s}^{-1}$; OH abstraction is not reported for the reactions of Yb^+ with the four other molecules with which it would be more exothermic (see Table 3). In fact, Yb^+ is unreactive with these molecules: $k < 5 \times 10^{-13} \text{ cm}^3 \text{ molecule}^{-1} \text{ s}^{-1}$ ^[8c,10] under FTICR conditions. We cannot completely rule out the possibility of an excited-state effect in this case, since it would require an excited-state population of only 0.4%.

2.5. Mechanism for O-Atom and OD Group Transfer

The delay of more than 50 kcal mol^{-1} in the onset of efficient exothermic O-atom transfer apparent in Figure 3 suggests the presence of kinetic barriers of perhaps this magnitude in the exothermic O-atom transfer reactions of Dy^+ , Ho^+ , Er^+ and Tm^+ with D_2O . Indeed, kinetic barriers have been reported for analogous dehydrogenation reactions of some first-row transition metal cations with water by Ugalde and co-workers,^[19] who used DFT (B3LYP functional) theory to evaluate the potential energy surfaces for these reactions. The path of these reactions is initiated by the formation of an $M(OH_2)^+$ complex ($M = \text{metal}$), which is followed by the stepwise migration of the two hydrogen atoms initially bonded to atomic oxygen to the metal centre before H_2 is finally eliminated. Although the overall O-atom transfer to these transition metal cations is often exothermic, the various calculated transition states are found to present substantial energy barriers, occasionally as large as 50 kcal mol^{-1} . A similar reaction mechanism with similar energy barriers for O-atom transfer from D_2O to atomic lanthanide cations accounts for the delayed onset in Figure 3.

The mechanism of OD transfer is expected to be more straightforward and may simply amount to D-OD bond insertion, in which the metal cation coordinates to the electronegative oxygen atom followed by the transfer of electron density and homolytic H-OH bond cleavage.

The mechanism advanced for the O-atom transfer observed with phenol, 2-propanol, ethanol and methanol is initiated with an OH or CO insertion, with the preferred insertion perhaps being determined by the relative O-H and C-O bond energies (see Table 3), and followed by four-centre electrocyclic elimination of RH .^[8c,10]

3. Conclusions

Lanthanide cations react with D_2O at room temperature in a helium bath at 0.35 Torr by O-atom transfer, OD transfer and D_2O addition. Our measurements show that D_2O is not highly reactive towards Ln^+ cations (reaction efficiency ≤ 0.14) and is less reactive than aliphatic alcohols and phenol. The reactivities of all of these molecules exhibit a periodic variation across the lanthanide series, with the early lanthanides in the "early" and "late" lanthanide series being the most reactive. With the exception of Lu^+ , a delay of more than 50 kcal mol^{-1} is observed in the onset of efficient exothermic O-atom transfer, which suggests the presence of kinetic barriers of perhaps this magnitude in the exothermic O-atom transfer reactions of Dy^+ , Ho^+ , Er^+ and Tm^+ with D_2O . O-atom transfer predominates in

the reactions of D₂O with the reactive lanthanide cations, and the efficiency of O-atom transfer correlates with the energy required to promote an electron to achieve a d¹s¹ or d² excited electronic configuration in which two non-f electrons are available for bonding. The efficiency of O-atom transfer decreases as the promotion energy increases, and the periodic trend in reaction efficiency along the lanthanide series matches the periodic trend in the corresponding electron-promotion energy. An Arrhenius-like correlation is observed for the dependence of reactivity on promotion energy for early lanthanide cations, and exhibits a characteristic temperature of 2600 ± 100 K.

D₂O is also an effective solvent of gas-phase LnO⁺ and LnOD⁺ cations which sequentially add up to five D₂O molecules in the higher-order chemistry that was observed under the experimental operating conditions of our ICP/SIFT tandem mass spectrometer.

Acknowledgments

Continued financial support from the Natural Sciences and Engineering Research Council of Canada is greatly appreciated. Also, we acknowledge support from the National Research Council, the Natural Science and Engineering Research Council and MDS SCIEX in the form of a Research Partnership grant. As holder of a Canada Research Chair in Physical Chemistry, D.K.B. thanks the contributions of the Canada Research Chair Program to this research.

Keywords: cations · gas-phase reactions · lanthanides · mass spectrometry · water chemistry

- [1] a) K. A. Gschneider, Jr., *Industrial Application of Rare Earth Elements*, American Chemical Society, Washington, DC, **1981**; b) Second International Conference on f-Elements, University of Helsinki, 1–6 August, **1994**.
- [2] D. K. Bohme in *The Encyclopedia of Mass Spectrometry*, vol. 4 (Eds.: M. L. Gross, R. M. Caprioli.), Elsevier, UK, **2005**, pp. 638–648.
- [3] a) Y. Huang, M. B. Wise, D. B. Jacobson, B. S. Freiser, *Organometallics* **1987**, *6*, 346–354; b) J. B. Schilling, J. L. Beauchamp, *J. Am. Chem. Soc.* **1988**, *110*, 15–24; c) L. S. Sunderlin, P. B. Armentrout, *Int. J. Mass Spectrom. Ion Process.* **1989**, *94*, 149–177.
- [4] J. L. Elkind, L. S. Sunderlin, P. B. Armentrout, *J. Phys. Chem.* **1989**, *93*, 3151–3158.
- [5] G. K. Koyanagi, D. K. Bohme, *J. Phys. Chem. A* **2001**, *105*, 8964–8968.
- [6] H. H. Cornehl, C. Heinemann, D. Schroeder, H. Schwarz, *Organometallics* **1995**, *14*, 992–999.
- [7] J. K. Gibson, *J. Phys. Chem.* **1996**, *100*, 15688–15694.
- [8] a) M. Azzaro, S. Breton, M. Decouzon, S. Geribaldi, *Int. J. Mass Spectrom. Ion Process.* **1993**, *128*, 1–20; b) S. Geribaldi, S. Breton, M. Decouzon, M. Azzaro, *J. Am. Soc. Mass Spectrom.* **1996**, *7*, 1151–1160; c) J. M. Carretas, J. Marcalo, A. Pires de Matos, *Int. J. Mass Spectrom.* **2004**, *234*, 51–61.
- [9] a) J. K. Gibson, R. G. Haire, *Radiochim. Acta* **2001**, *89*, 709–719; b) W. W. Yin, A. G. Marshall, J. Marcalo, A. Pires de Matos, *J. Am. Chem. Soc.* **1994**, *116*, 8666–8672.
- [10] J. M. Carretas, A. Pires de Matos, J. Marcalo, M. Pissavini, M. Decouzon, S. Geribaldi, *J. Am. Soc. Mass Spectrom.* **1998**, *9*, 1035–1042.
- [11] N. Marchande, S. Breton, S. Geribaldi, J. M. Carretas, A. Pires de Matos, J. Marcalo, *Int. J. Mass Spectrom.* **2000**, *195/196*, 139–148.
- [12] M. D. Vieira, J. Marcalo, A. Pires de Matos, *J. Organomet. Chem.* **2001**, *632*, 126–132.
- [13] G. K. Koyanagi, X. Zhao, V. Blagojevic, M. J. Y. Jarvis, D. K. Bohme, *Int. J. Mass Spectrom.* **2005**, *241*, 189–196.
- [14] X. Zhao, G. K. Koyanagi, D. K. Bohme, *Can. J. Chem.* **2005**, *83*, 1839–1846.
- [15] J. K. Gibson, *J. Phys. Chem. A* **2003**, *107*, 7891–7899.
- [16] a) T. F. Magnera, D. E. David, J. Michl, *J. Am. Chem. Soc.* **1989**, *111*, 4100–4101; b) Y.-M. Chen, D. E. Clemmer, P. B. Armentrout, *J. Phys. Chem.* **1994**, *98*, 11490–11498; c) M. Sanekata, F. Misaizu, K. Fuke, S. Iwata, K. Hashimoto, *J. Am. Chem. Soc.* **1995**, *117*, 747–754; d) R. S. MacTaylor, W. D. Vann, A. W. Castleman, Jr., *J. Phys. Chem.* **1996**, *100*, 5329–5333; e) V. A. Mikhailov, P. E. Barran, A. J. Stace, *Phys. Chem. Chem. Phys.* **1999**, *1*, 3461–3465; f) G. K. Koyanagi, D. K. Bohme, I. Kretzschmar, D. Schroeder, H. Schwarz, *J. Phys. Chem. A* **2001**, *105*, 4259–4271.
- [17] R. Johnsen, H. L. Brown, M. A. Biondi, *J. Chem. Phys.* **1971**, *55*, 186–188.
- [18] a) N. F. Dalleska, K. Honma, L. S. Sunderlin, P. B. Armentrout, *J. Am. Chem. Soc.* **1994**, *116*, 3519–3528; b) D. E. Clemmer, Y.-M. Chen, F. A. Khan, P. B. Armentrout, *J. Phys. Chem.* **1994**, *98*, 6522–6529; c) D. E. Clemmer, Y.-M. Chen, N. Aristov, P. B. Armentrout, *J. Phys. Chem.* **1994**, *98*, 7538–7544; d) Y.-M. Chen, D. E. Clemmer, P. B. Armentrout, *J. Am. Chem. Soc.* **1994**, *116*, 7815–7826.
- [19] a) A. Irigoras, J. E. Fowler, J. M. Ugalde, *J. Am. Chem. Soc.* **1999**, *121*, 574–580; b) A. Irigoras, J. E. Fowler, J. M. Ugalde, *J. Am. Chem. Soc.* **1999**, *121*, 8549–8558; c) A. Irigoras, O. Elizalde, I. Silanes, J. E. Fowler, J. M. Ugalde, *J. Am. Chem. Soc.* **2000**, *122*, 114–122.
- [20] P. Cheng, G. K. Koyanagi, D. K. Bohme, unpublished results.
- [21] a) G. K. Koyanagi, V. I. Baranov, S. D. Tanner, D. K. Bohme, *J. Anal. Atom. Spectrom.* **2000**, *15*, 1207–1210; b) G. K. Koyanagi, V. V. Lavrov, V. Baranov, D. Bandura, S. Tanner, J. W. McLaren, D. K. Bohme, *Int. J. Mass Spectrom.* **2000**, *194*, L1–L5.
- [22] T. Su, W. J. Chesnavich, *J. Chem. Phys.* **1982**, *76*, 5183–5185.
- [23] A. A. Maryott, F. Buckley, *National Bureau of Standards Circular (U.S.)* **1953**, *53*, 29.
- [24] T. R. Dyke, J. S. Muentner, *J. Chem. Phys.* **1973**, *59*, 3125–3127.
- [25] <http://webbook.nist.gov/chemistry/>.
- [26] *CRC Handbook of Chemistry and Physics, 82nd ed.* (Ed.: D. R. Lide), CRC Press, Boca Raton, FL, **2001**.
- [27] S. G. Lias, J. E. Bartmess, J. F. Liebman, J. L. Holmes, R. D. Levin, W. G. Mallard, *J. Phys. Chem. Ref. Data.* **1988**, *17*, 1–861.

Received: April 18, 2006

Published online on June 29, 2006